ISSN No:-2456-2165 https://doi.org/10.38124/ijisrt/26jun532

Experimental Investigation of Flexural Behaviour, Tensile Strength, and Crack Pattern Characteristics of BFRP-Reinforced Concrete Beams

Nivrutti R. Savandre[1]; Sandip A. Karale[2]; Santosh T. Sanap[2]

[1]Student of Masters in Engineering (Structure) JES's S. N. D. College of Engineering & Research Center, Yeola, Lecturer in Civil Engineering Department at SNJB's Shir Hiralal Hastimal (Jain Brothers Jalgaon) Polytechnic, Chandwad

[2]Assistant Professor JES's S. N. D. College of Engineering & Research Center, Yeola

Publication Date: 2026/06/30

Abstract: Basalt Fiber Reinforced Polymer (BFRP) bars have emerged as a promising alternative to conventional steel reinforcement owing to their excellent corrosion resistance, high tensile strength, and lightweight characteristics. The present investigation evaluates the tensile and flexural behaviour of reinforced concrete beams reinforced with BFRP bars and compares their performance with that of conventional steel-reinforced beams. Tensile tests were conducted on BFRP bars using a Universal Testing Machine to determine their mechanical properties, while flexural behaviour was examined through four-point bending tests on beam specimens. The influence of reinforcement type and reinforcement ratio on load-carrying capacity, deflection response, crack development, and failure characteristics was investigated. Analytical predictions based on ACI 440 provisions and finite element simulations performed using ANSYS were employed to validate the experimental findings. The results indicated that BFRP-reinforced beams exhibited larger deflections and wider crack widths than steel-reinforced beams because of the lower elastic modulus and linear elastic nature of BFRP bars. However, increasing the reinforcement ratio significantly enhanced flexural stiffness and ultimate load capacity. A satisfactory agreement was observed among experimental observations, analytical calculations, and numerical simulations. The findings demonstrate that BFRP bars can effectively replace conventional steel reinforcement in structures requiring superior durability and corrosion resistance.

Keywords: *Basalt Fiber Reinforced Polymer, Reinforced Beam, Flexural Behaviour, Tensile Behaviour, ACI 440, ANSYS, Finite Element Analysis.*

How to Cite: Nivrutti R. Savandre; Sandip A. Karale; Santosh T. Sanap (2026) Experimental Investigation of Flexural Behaviour, Tensile Strength, and Crack Pattern Characteristics of BFRP-Reinforced Concrete Beams. *International Journal of Innovative Science and Research Technology*, 11(6), 1702-1713. https://doi.org/10.38124/ijisrt/26jun532

I. INTRODUCTION

Reinforced concrete (RC) structures located in marine and coastal regions are frequently subjected to severe environmental conditions, including elevated humidity, chloride ingress, and exposure to seawater spray. These aggressive factors accelerate the corrosion of embedded reinforcement, which is one of the primary causes of deterioration in coastal RC bridges and buildings [1,2]. The corrosion process significantly affects both the durability [3] and the structural integrity of such components [4,5]. Since corrosion-related damage leads to considerable repair and maintenance expenses [6,7], the use of corrosion-resistant reinforcement has become essential for ensuring the long-term serviceability and sustainability of marine RC structures. Various approaches have been explored to mitigate reinforcement corrosion, including the use of corrosion inhibitors [8,9] and protective coatings on steel bars [10,11]. Nevertheless, these techniques often involve additional complexity, higher costs, and limited effectiveness, making them insufficient for completely eliminating the problem of steel corrosion recent developments have demonstrated that replacing conventional steel reinforcement with fiber-reinforced polymer (FRP) bars in concrete structures offers an efficient solution to corrosion-related deterioration [12–14]. Owing to their low weight, high tensile strength, excellent resistance to corrosion and fatigue, and superior electromagnetic insulation properties, FRP materials have emerged as attractive alternatives to traditional steel reinforcement [15,16]. These characteristics make FRP composites highly

ISSN No:-2456-2165 https://doi.org/10.38124/ijisrt/26jun532

suitable for structures exposed to aggressive environments [19].

Despite these advantages, the extensive use of FRP bars remains restricted by two inherent limitations, namely their relatively low elastic modulus and lack of yielding behaviour. Because FRP reinforcement exhibits linear elastic characteristics up to failure, FRP-reinforced concrete beams generally experience brittle failure without noticeable warning. Furthermore, the lower stiffness of FRP bars compared with steel results in larger deflections and wider crack widths for members possessing identical reinforcement ratios. Consequently, the design of FRP-reinforced concrete members is often governed by serviceability considerations rather than ultimate strength requirements [20–22].

Among the various FRP materials, basalt fiber-reinforced polymer (BFRP) has gained increasing attention in recent years due to its cost-effectiveness and favorable mechanical properties compared with conventional glass FRP (GFRP) and carbon FRP (CFRP) systems [23,24]. Nevertheless, improving the brittle behaviour of BFRP-reinforced flexural members remains a major challenge. The enhancement of ductility in FRP-reinforced concrete structures largely depends on increasing the ultimate compressive strain of concrete, thereby postponing concrete crushing and enabling the FRP bars to sustain higher stress levels.

To overcome this limitation, numerous researchers have investigated the incorporation of randomly distributed discrete fibers into concrete. For example, [25] reported that the addition of polypropylene fibers improved the ductility of FRP-reinforced beams by more than 30%, exceeding the minimum ductility requirements. According to [26], short basalt fibers had little influence on compressive strength but noticeably enhanced the flexural modulus of concrete. Similarly, [27] observed that steel fiber incorporation increased the cracking load, ultimate flexural capacity, and ductility of high-strength FRP-RC beams while simultaneously reducing crack widths. In another study, [28] evaluated the effects of different fiber types on GFRP-reinforced concrete beams and concluded that fiber addition improved ductility without compromising flexural performance. Focusing specifically on basalt fibers, [29] demonstrated that their inclusion in BFRP-reinforced concrete beams effectively controlled crack propagation and enhanced curvature ductility.

Collectively, these investigations highlight the capability of fiber-reinforced concrete, particularly basalt fiber-reinforced concrete, to alleviate the brittle failure behaviour associated with FRP-reinforced members. However, research concerning the flexural response of basalt fiber-reinforced concrete (BFRC) beams reinforced with BFRP bars remains limited. Moreover, current design recommendations and standards for FRP-reinforced concrete structures [16,30] do not explicitly address the application of BFRP reinforcement. Therefore, the present study aims to evaluate the flexural behaviour of BFRC beams reinforced with either steel or BFRP bars through experimental investigation, analytical assessment, and finite element modeling.

➢ *The Objectives of the Present Investigation are as Follows:*

- To evaluate the tensile properties and stress–strain characteristics of BFRP bars through experimental testing in accordance with Indian Standard (IS) recommendations.
- To investigate the flexural behaviour of reinforced concrete beams reinforced with BFRP and conventional steel bars under four-point loading conditions.
- To assess the influence of reinforcement type and reinforcement ratio on crack propagation, stiffness degradation, deformation characteristics, and ultimate load-carrying capacity.
- To develop analytical models based on ACI 440 recommendations and validate the experimental results through finite element simulations using ANSYS.

II. SET-UP FOR EXPERIMENTS

In the present study, the flexural response of concrete beams reinforced with BFRP bars was examined under gradually increasing loads using a four-point bending test arrangement, as shown in Fig. 1. The experimental program was designed to evaluate the behaviour of the specimens throughout the loading process and included the preparation, testing, and analysis of beam specimens subjected to controlled flexural loading. measuring the mid-span deflection of the beam specimens using Linear Variable Differential Transformers (LVDTs). Strain measurements were recorded at the mid-span section by positioning strain gauges at the tension zone of the beam. Crack initiation and crack propagation patterns were carefully monitored throughout the loading process, and crack widths were measured using a Vernier caliper with proper crack numbering and identification at different loading stages.

ISSN No:-2456-2165 https://doi.org/10.38124/ijisrt/26jun532

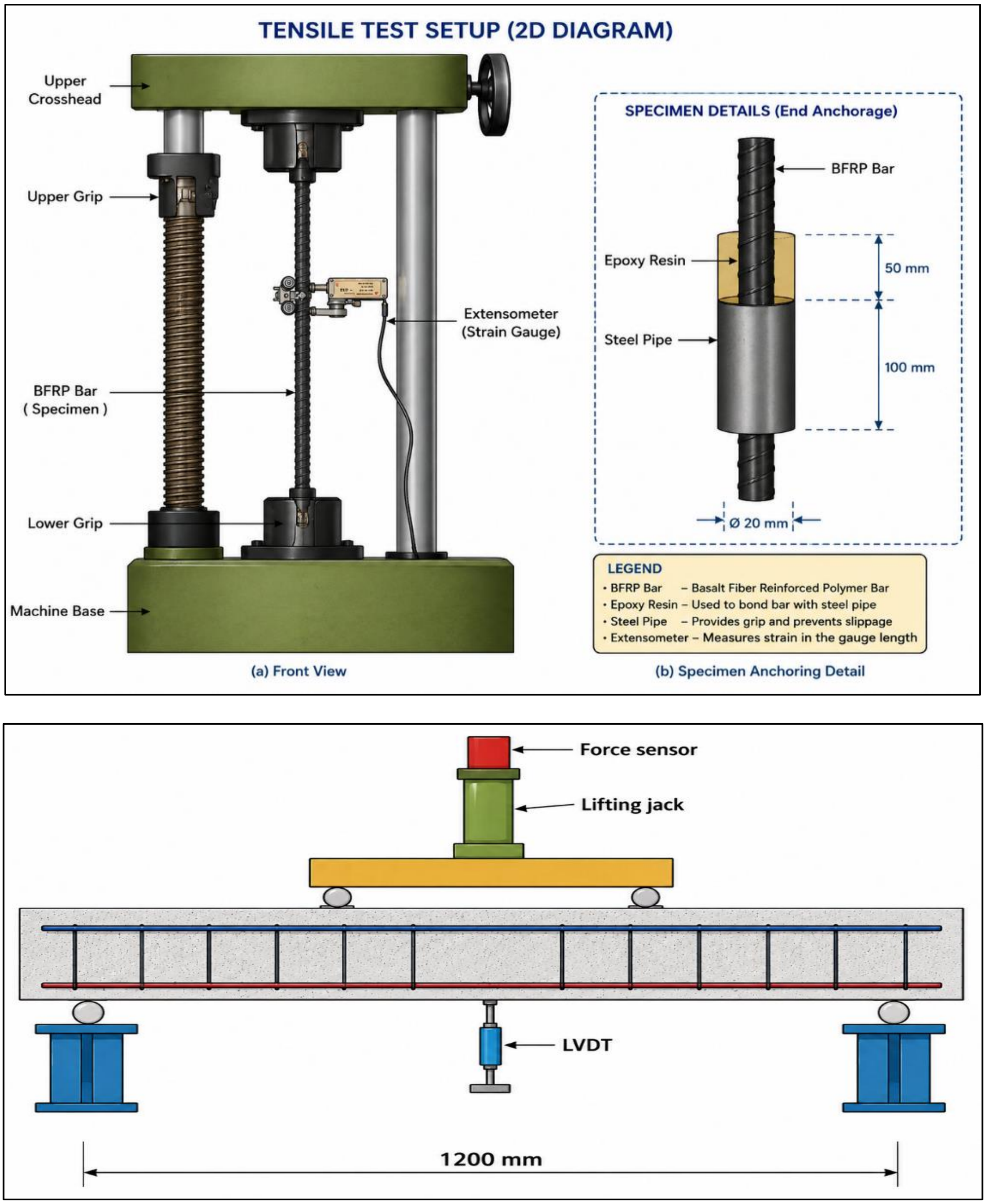

Fig 1 Experimental Setup.

➢ *Material Properties*

As shown in Fig. 2, BFRP bars were used as longitudinal reinforcement in this study to evaluate their mechanical and structural behaviour in reinforced concrete beams. A total of six BFRP-reinforced beam specimens and three conventionally steel-reinforced beam specimens were cast and tested for comparative evaluation. Prior to beam testing, tensile tests were conducted on BFRP bar specimens using a Universal Testing Machine (UTM) to determine their mechanical properties, including tensile strength and elastic modulus. For proper gripping during tensile testing, both ends of the BFRP bars were anchored inside steel pipes using epoxy resin to prevent premature crushing and slippage of the specimens during loading, as shown in Fig. 3. The experimental observations indicated that BFRP bars exhibited linear elastic behaviour up to failure without any yielding phenomenon, unlike conventional steel reinforcement. Compared with steel bars, BFRP bars demonstrated higher tensile strength but lower elastic modulus, which resulted in comparatively larger deflections and wider crack widths under loading conditions. Steel-reinforced beam specimens were considered as control specimens for evaluating the flexural and serviceability behaviour of BFRP-reinforced concrete beams.

ISSN No:-2456-2165 https://doi.org/10.38124/ijisrt/26jun532

Fig 2 Characteristic of BFRP.

Fig 3 Tensile Test Specimen

- *Specimen Design*

BFRP tensile specimens were prepared using steel pipe–epoxy anchorages in accordance with ASTM D7205 to avoid grip-induced damage and slippage. Mild steel pipes of 20 mm internal diameter and 300 mm anchorage length were used at both ends of 12 mm BFRP bars to ensure effective stress transfer and failure within the gauge length. A 500 mm gauge length was adopted, resulting in a total

ISSN No:-2456-2165 https://doi.org/10.38124/ijisrt/26jun532

specimen length of 1100 mm. A two-component structural epoxy resin was used for anchorage bonding, and specimens were cured for 48 hours before testing. Gripping was applied only on steel pipes to ensure pure axial loading and test validity.

A total of six beam specimens with dimensions of 1200 mm × 150 mm × 250 mm were fabricated for the experimental investigation. The beams were reinforced in tension using either HYSD 500 steel bars or BFRP bars with diameters of 10 mm and 12 mm. A uniform concrete cover of 30 mm was provided to all specimens. The detailed specifications of the beams are summarized in Table 1. In Table 2, ρf ρ is the actual reinforcement ratio represents the actual reinforcement ratio, whereas, ρ1 denotes the equivalent nominal reinforcement ratio obtained based on strength conversion. The balanced reinforcement ratio, was evaluated according to the procedure recommended. To investigate different failure mechanisms, the BFRP-reinforced BFRC beams were designed with reinforcement ratios both below and above the balanced value, resulting in under-reinforced and over-reinforced specimens, respectively.

III. ANALYSIS AND DISCUSSION OF EXPERIMENTAL FINDINGS

➢ *Tensile Strength of BFRP*

Tensile testing of 10 mm and 12 mm diameter Basalt Fiber Reinforced Polymer (BFRP) bars was carried out using a Universal Testing Machine (UTM) in accordance with ASTM D7205 recommendations for FRP reinforcement bars. Three specimens of each diameter were tested to evaluate the tensile behaviour and mechanical properties of the reinforcement. The experimental results indicated that the tensile strength of 10 mm diameter BFRP bars ranged from 974 MPa to 1122 MPa, with an average tensile strength of 1048 MPa. Similarly, the tensile strength of 12 mm diameter BFRP bars varied between 959 MPa and 1137 MPa, with an average value of 1049 MPa. The elastic modulus obtained from testing ranged between 46 GPa and 50 GPa for both bar diameters, Detailed data is presented in Table 1 which is consistent with values reported in previous research literature and ACI 440 recommendations. All specimens exhibited nearly linear elastic behaviour up to failure without yielding, followed by sudden brittle rupture, which is characteristic of FRP reinforcement materials. The obtained results confirm that BFRP bars possess high tensile strength and satisfactory mechanical performance suitable for structural applications in reinforced concrete members.

Table 1 Tensile Test Results of BFRP Bars

Specimen No.	Diameter of Rebar (mm)	Ultimate Load (kN)	Cross-sectional Area (mm²)	Elongation (mm)	Tensile Strength (MPa)	Elastic Modulus (GPa)	Mode of Failure
BFRP-10-1	10	76.5	78.54	7.8	974	46.2	Brittle rupture
BFRP-10-2	10	88.1	78.54	8.7	1122	49.1	Brittle rupture
BFRP-10-3	10	82.4	78.54	8.2	1049	47.8	Brittle rupture
BFRP-12-1	12	118.8	113.10	9.3	1050	48.3	Brittle rupture
BFRP-12-2	12	108.5	113.10	8.9	959	46.5	Brittle rupture
BFRP-12-3	12	128.6	113.10	9.8	1137	49.8	Brittle rupture

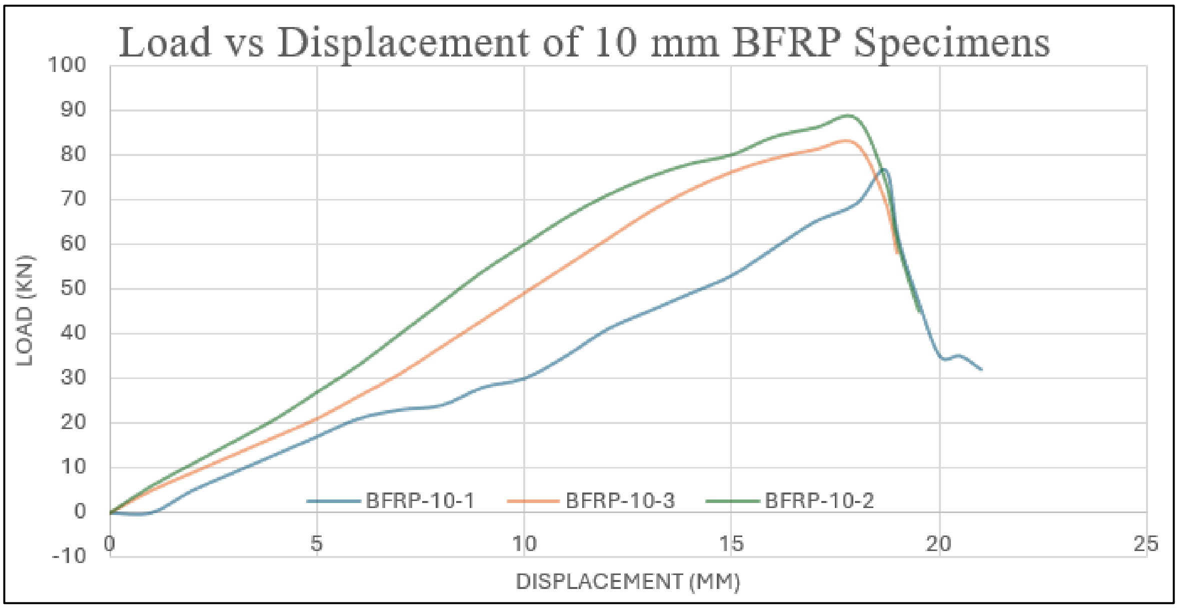

ISSN No:-2456-2165 https://doi.org/10.38124/ijisrt/26jun532

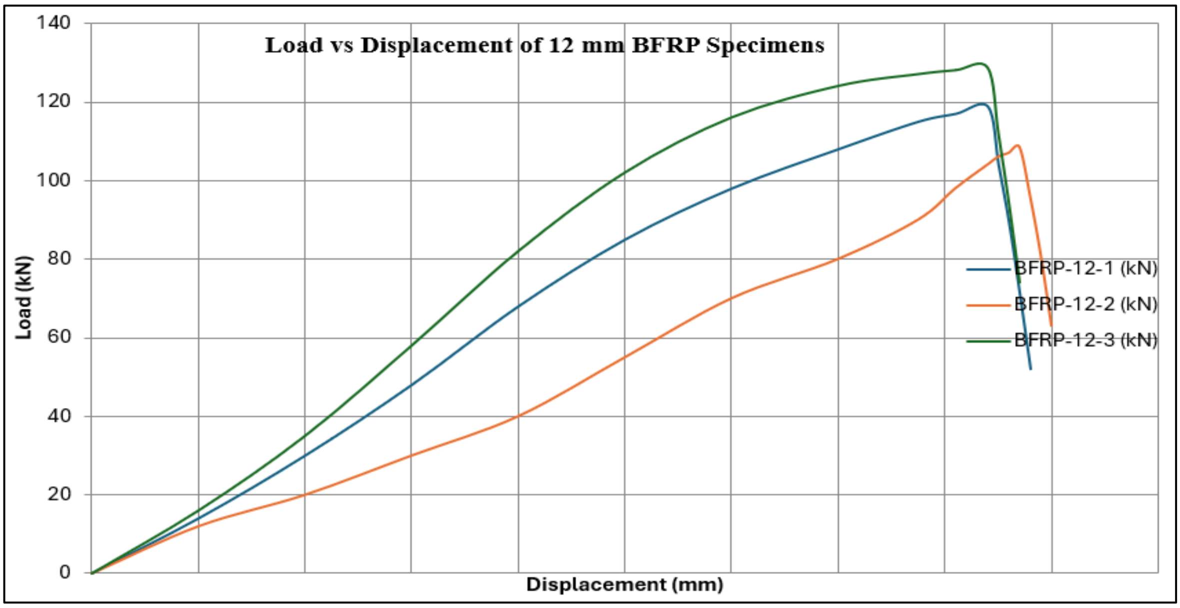

Fig 4 Load Vs Displacement of BFRP

- ➢ *Deflection Behaviour*

The measured strain profiles along the depth of both steel-reinforced and BFRP-reinforced concrete beams exhibited an approximately linear distribution throughout the loading process, confirming the validity of the plane section hypothesis. A clear distinction was observed in the moment–deflection behaviour of beams reinforced with BFRP bars and those reinforced with conventional steel bars. The load–deflection curves of BFRP-reinforced specimens showed a characteristic bilinear response. A noticeable decrease in flexural stiffness occurred immediately after the initiation of cracking. Beyond this stage, the beams maintained an almost linear elastic response until failure, without exhibiting any yielding behaviour, which reflects the relatively low ductility associated with BFRP reinforcement. This response can be attributed to the linear elastic characteristics and lower modulus of elasticity of BFRP bars in comparison with steel reinforcement.

Among all specimens, beams reinforced with 10 mm diameter BFRP bars experienced the largest deflections and crack widths owing to their lower reinforcement ratio and reduced stiffness. The average ultimate mid-span deflection of these beams was approximately 25 mm. In contrast, specimens reinforced with 12 mm BFRP bars recorded smaller deflections in the range of 18–19 mm. Steel-reinforced beams, however, exhibited the conventional three-stage response consisting of an initial uncracked elastic region, followed by stiffness degradation after cracking and subsequent yielding before reaching ultimate failure. The average maximum deflection of steel-reinforced specimens was nearly 12 mm, which was considerably lower than that observed in the BFRP-reinforced members. In terms of cracking behaviour, the BFRP-reinforced beams developed wider flexural cracks, with crack widths varying between 2 and 3 mm, whereas the corresponding values for steel-reinforced beams remained below 1 mm. The experimental observations obtained in the present study are consistent with previously reported findings in the literature, where BFRP-reinforced concrete members were shown to exhibit larger deflections, increased crack widths, and predominantly brittle failure modes. These characteristics are mainly associated with the comparatively lower stiffness and absence of yielding in FRP reinforcement systems.

Table 2 Main Design Parameters of Beam Specimens

Beam Specimen	Longitudinal Reinforcement	Longitudinal Reinforcement Area (mm²)	Reinforcement Ratio ρ (%)
2B10-1	2B10	157.0	0.41
2B10-2	2B10	157.0	0.41
2B12-1	2B12	226.2	0.59
2B12-2	2B12	226.2	0.59
3A16-1	3A16	603	1.61
2A20-2	2A20	2628	1.67

A = HYSD 500 B= BFRP ρ = Provided Reinforcement Ratio

Table 3 Mechanical Properties of Steel Bars.

Steel	D (mm)	fy (MPa)	fu (MPa)
HYSD 500	16	500	545
	20	500	545

ISSN No:-2456-2165 https://doi.org/10.38124/ijisrt/26jun532

Table 4 Mechanical Properties of BFRP.

Steel	D (mm)	E_{fp} (GPa)	F_{fp} (MPa)
BFRP	10	50	1122
	12	50	1137

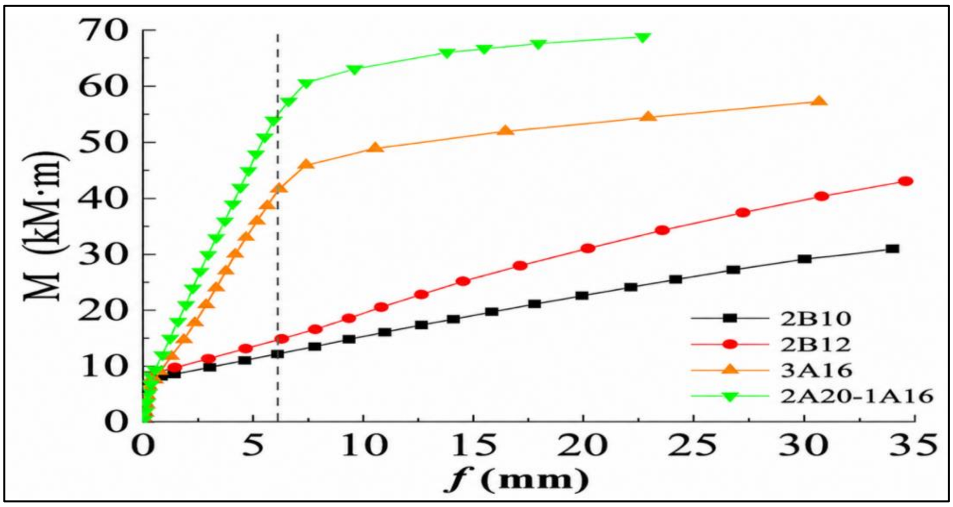

Fig 5 Moment Deflection Curve of the Tested Beam

Table 5 Bending Behaviour of BFRP and Steel Reinforced Beams

Beam Specimen	*Ultimate Moment, Mu (kN·m)*	*Deflection at 0.3Mu,sc (mm)*	*Deflection at 0.5Mu,sc (mm)*	*Deflection at 0.7Mu,sc (mm)*
2B12	41.7	9.85	18.93	27.45
3A16	53.4	2.19	3.91	5.61

➢ *Cracking Moment*

The experimentally determined cracking moments of the beam specimens varied from 7.1 to 9.5 kN·m, yielding an average value of 8.3 kN·m. The relatively small variation among the specimens was anticipated, since the onset of cracking is primarily governed by the tensile strength of concrete, which remained essentially constant throughout the experimental program.

Table 5 presents a comparison between the measured cracking moments and the corresponding values calculated according to the provisions of ACI 440.1R-15 [16]. The ratio between the predicted and experimentally obtained cracking moments was found to be 1.17 ± 0.06. In all cases, the analytical predictions provided by the ACI model were greater than the measured values, indicating that the code tends to slightly overestimate the cracking moment of the tested beams.

The cracking and ultimate moment capacities of the tested beams were evaluated experimentally and compared with analytical and finite element predictions. The BFRP reinforced beams exhibited lower flexural stiffness and ultimate moment capacity compared to steel reinforced beams; however, they demonstrated stable flexural behaviour up to brittle failure. The steel reinforced beams, namely 3A16 and 2A20, exhibited higher cracking and ultimate moments due to the superior stiffness and yielding characteristics of steel reinforcement. The predicted-to-experimental ratios obtained from ACI provisions, theoretical calculations, and finite element analysis showed satisfactory agreement with the experimental results, with average values remaining close to unity. The comparison confirms the reliability of the adopted analytical procedures for predicting the flexural behaviour of both BFRP and steel reinforced concrete beams.

Table 6 Cracking and Ultimate Moments

Beam Specimen	Experimental Cracking Moment Mcr (kN·m)	Experimental Ultimate Moment Mu (kN·m)	Mcr (ACI)	Mcr (Theory)	Mcr (FE)	Mu (ACI)	Mu (Theory)	Mu (FE)
2B10-1	6.8	31.2	1.19	0.98	1.04	1.08	1.03	1.02
2B10-2	7.2	32.5	1.16	0.96	1.03	1.06	1.04	1.01
2B12-1	7.9	43.8	1.14	0.97	1.05	1.10	1.02	1.00
2B12-2	8.1	45.2	1.12	0.95	1.04	1.11	1.03	1.04
3A16-1	8.8	54.6	1.08	1.01	1.06	0.99	1.00	0.98
2A20-1	9.3	67.2	1.06	1.00	1.09	0.98	1.01	1.00
Average Value.	—	—	1.12	0.98	1.05	1.05	1.02	1.01
Coefficient of Variation.	—	—	0.049	0.027	0.032	0.058	0.031	0.033

ISSN No:-2456-2165 https://doi.org/10.38124/ijisrt/26jun532

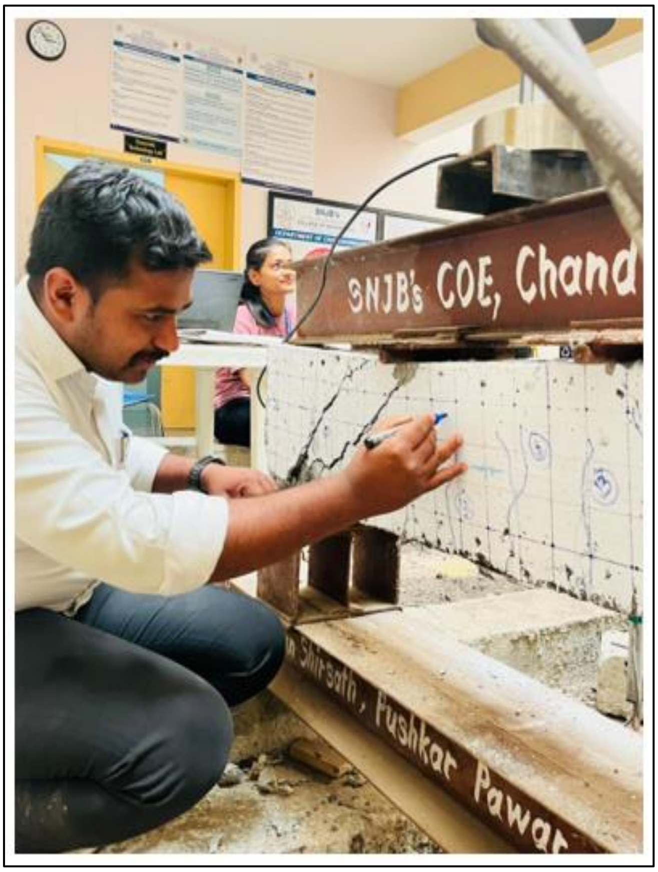

Fig 6 Beam Specimen after Test

IV. THEORETICAL ANALYSIS OF FLEXURAL BEHAVIOUR OF BFRP REINFORCED CONCRETE BEAMS

➢ *Analytical Model for Flexural Behaviour of BFRP Reinforced Beams*

The moment–deflection behaviour of BFRP reinforced concrete beams was analytically evaluated using strain compatibility, force equilibrium, and constitutive relationships of concrete and BFRP reinforcement. The analytical procedure adopted in the present study was developed based on previously published analytical models for FRP reinforced concrete beams and modified according to the experimental properties of the tested BFRP bars.

The BFRP bars were assumed to behave as a perfectly linear elastic material up to failure. The constitutive relationship of BFRP reinforcement is expressed as:

$$\sigma_{fp} = E_{fp}\varepsilon_{fp}$$

Where:

σ_{fp} = stress in BFRP bars

E_{fp} = elastic modulus of BFRP bars

ε_{fp} = strain in BFRP bars

The experimentally obtained tensile properties of BFRP reinforcement used in the present study were the stress–strain behaviour of concrete in compression was assumed according to IS 456:2000 provisions, while concrete in tension was neglected after cracking.

Table 7 Properties of BFRP Reinforcement

Property	10 mm BFRP	12 mm BFRP
Tensile Strength	1048 MPa	1049 MPa
Elastic Modulus	47.7 GPa	48.2 GPa

➢ *Section Analysis of Flexural Behaviour*

Based on experimental observations, the flexural response of BFRP reinforced beams can be divided into three stages:

Table 8 Experimental Observations

Stage	Behaviour
Elastic Stage	Uncracked section with linear elastic behaviour
Service Stage	Cracking in tensile zone with reduced stiffness
Failure Stage	Concrete crushing or BFRP rupture

Initially, the beam remained uncracked and exhibited nearly linear elastic behaviour. As the applied load increased, flexural cracks initiated at the tension zone near the mid-span region. After cracking, the stiffness of the beam decreased significantly due to the lower elastic modulus of BFRP bars. Finally, failure occurred when either

ISSN No:-2456-2165 https://doi.org/10.38124/ijisrt/26jun532

the concrete compressive strain approached its ultimate value or the BFRP reinforcement reached rupture strain.

The strain distribution across the beam depth remained approximately linear throughout the loading stages, thereby validating the plane section assumption for BFRP reinforced concrete beams.

- *Elastic Stage*

At the elastic stage, the tensile concrete remained uncracked and both concrete and BFRP reinforcement behaved elastically.

The cracking moment was calculated using:

$$M_{cr} = \frac{f_r I_g}{y_t}$$

Where:

$f_r =$ modulus of rupture of concrete
$I_g =$ gross moment of inertia
$y_t =$ distance from neutral axis to tension face
The modulus of rupture of concrete was determined as:

$$f_r = 0.62\sqrt{fck}$$

- *Service Stage with Cracks*

After cracking, the concrete in the tensile zone was neglected and tensile force was resisted primarily by the BFRP reinforcement.

The force equilibrium equation is expressed as:

$$0.85\, f_{ck}\, bx = A_{fp} f_{fp}$$

Where:

$A_{fp} =$ area of BFRP reinforcement
$f_{fp} = stress\ in\ BFRP\ bars$
$x = neutral\ axis\ depth$

The corresponding flexural moment capacity was calculated as:

$$M = A_{fp} f_{fp}\left(d - \frac{\propto}{2}\right)$$

Where:

$$\propto = \beta_1\, x$$

- *Failure Stage*

At ultimate stage, the BFRP reinforced beams exhibited brittle flexural failure without yielding of reinforcement. The failure occurred due to either:

✓ Crushing of concrete in compression zone, or
✓ Rupture of BFRP reinforcement.

The tested BFRP beams exhibited nearly bilinear moment–deflection behaviour with significant reduction in stiffness after cracking. Unlike steel reinforced beams, no yielding plateau was observed because of the linear elastic nature of BFRP reinforcement.

The 10 mm BFRP beams exhibited larger mid-span deflection and wider crack widths compared to the 12 mm BFRP and steel reinforced beams due to the lower reinforcement ratio and reduced flexural stiffness.

➢ *Mid-Span Deflection Calculation*

The mid-span deflection of simply supported beams subjected to two-point loading was calculated using:

$$f = S\,\phi\, l^2$$

Where:

$$f = \text{mid} - \text{span deflection}$$

$$S = loading\ coefficient$$

$$\phi = section\ curvature$$

$$l = effective\ span\ of\ beam$$

The curvature was determined from:

$$\phi = \frac{\varepsilon_{fcs}}{h - c}$$

The analytical results indicated that BFRP reinforced beams developed significantly higher deflections compared to steel reinforced beams due to the lower elastic modulus of BFRP reinforcement.

➢ *Simple Method for Flexural Capacity*

The flexural capacity of BFRP reinforced beams was also evaluated using simplified ACI 440 provisions. The effective stress block parameter was calculated as:

$$\beta 1 = 0.85 - 0.05\left(\frac{fc' - 28}{7}\right) \geq 0.65$$

The analytical predictions showed good agreement with the experimental results, with predicted-to-experimental ratios remaining close to unity.

➢ *Simplified Method for Deflection*

The effective moment of inertia recommended by ACI 440.1R was used to calculate beam deflection:

$$I_e = I_{cr}\left[\frac{1}{1 - \gamma (M_{cr}/M)^2 (1 - I_{cr}/I_g)}\right]$$

The calculated moment–deflection curves closely matched the experimental response of the tested beams, thereby validating the applicability of the simplified ACI method for BFRP reinforced concrete beams.

ISSN No:-2456-2165 https://doi.org/10.38124/ijisrt/26jun532

➢ *Crack Width Calculation*

The crack width of BFRP reinforced beams was determined according to ACI 440 recommendations:

$$\omega = 2 \frac{f_f}{E_{fp}} k_b \sqrt{d_c^2 + \frac{s^2}{4}}$$

Where:

k_b = bond coefficient
d_c = concrete cover thickness
s = reinforcement spacing
f_f = stress in BFRP bars

The analytical crack width predictions showed satisfactory agreement with the experimentally measured crack widths.

V. FE SIMULATION

➢ *Finite Element Model*

In the finite element investigation of BFRP-reinforced beams, the constitutive relationships adopted for both BFRP and steel reinforcement were identical to those employed in the analytical study. The plastic damage parameters assigned to the basalt fiber-reinforced concrete (BFRC) are summarized in Table 7. Numerical simulations were carried out using the finite element package ANSYS. In the developed model, the concrete body was represented by three-dimensional solid elements (C3D8R), whereas the reinforcing bars were modelled using truss elements (T3D2). To avoid stress concentration and local crushing effects beneath the loading pads, the cushion blocks were assumed to behave as linear elastic materials possessing a relatively high modulus of elasticity. A mesh size of 50 × 50 mm was adopted, resulting in a discretization consisting of 11,128 C3D8R elements and 731 T3D2 elements. Since mesh density influences the accuracy of numerical predictions, a detailed mesh sensitivity study is recommended for future investigations to improve the reliability of the analysis. Perfect bond conditions were assumed between the reinforcement and the surrounding BFRC, implying that no slip occurred at the interface throughout the loading history.

➢ *Numerical Results*

The moment–deflection responses obtained from finite element analysis The comparison demonstrated satisfactory agreement between the numerical predictions and test observations over the entire loading range for all beam specimens. Furthermore, Table 6 presents the comparison of the simulated and experimentally obtained values of cracking moment and ultimate moment. The numerical model provided predictions that closely matched the experimental results. The average ratio between the predicted and measured cracking moments for all specimens was 1.07 ± 0.034, while the corresponding ratio for the ultimate moments was 1.00 ± 0.036. These results confirm the capability of the developed finite element model to accurately reproduce the flexural behaviour and load-carrying capacity of the tested beams.

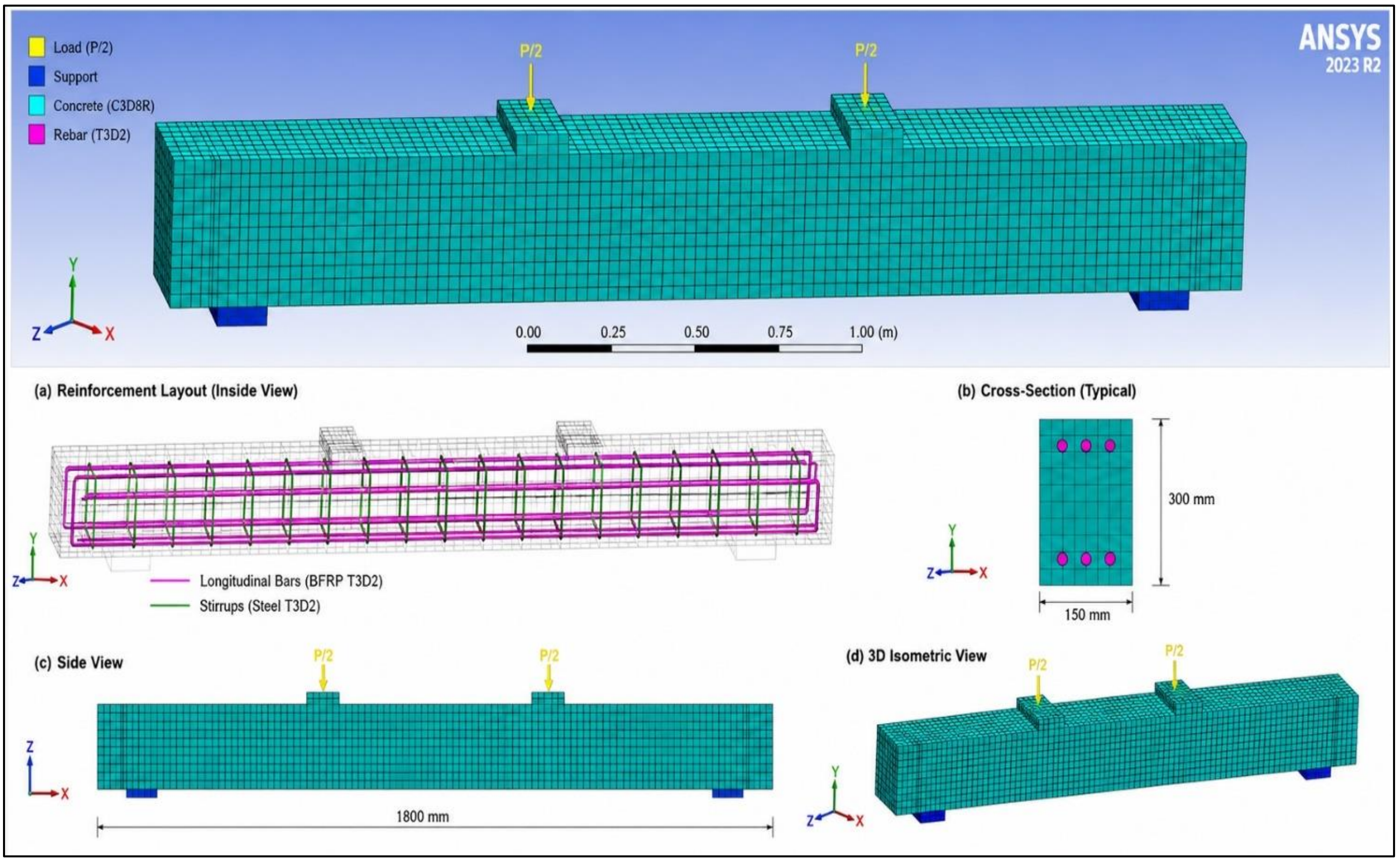

Fig 7 Finite Element Model

ISSN No:-2456-2165 https://doi.org/10.38124/ijisrt/26jun532

Table 9 Plastic Damage Parameters of BFRP Beam [36].

Expansion angle	Eccentricity	f_{b0}/f_{co}	k	Viscosity coefficient
40	0.10	1.66	0.677	0.0005

VI. CONCLUSIONS

This study investigated the flexural behaviour of reinforced concrete beams reinforced with BFRP bars and conventional steel bars through experimental testing, theoretical analysis, and finite element simulation. Based on the obtained results, the following conclusions can be drawn

- The load–deflection response of BFRP-reinforced concrete beams exhibited a characteristic bilinear behaviour, which can be attributed to the linear elastic nature of BFRP bars. Prior to crack initiation, all specimens possessed comparable flexural stiffness. Following cracking, a marked reduction in stiffness was observed because of the relatively low modulus of elasticity of BFRP reinforcement. Increasing the bar diameter and reinforcement ratio enhanced the post-cracking stiffness and contributed to better crack control.
- Steel-reinforced concrete beams displayed the conventional three-stage flexural response, comprising an initial elastic stage, a reduction in stiffness after cracking, and yielding of reinforcement before failure. Owing to the higher stiffness and ductile characteristics of steel, these beams experienced smaller deflections and narrower cracks than their BFRP-reinforced counterparts.
- In comparison with steel-reinforced beams possessing similar reinforcement capacities, BFRP-reinforced specimens showed lower flexural rigidity, greater mid-span deflections, and more pronounced crack widths. Beams reinforced with 10 mm BFRP bars exhibited the largest deformation and crack propagation due to their lower reinforcement ratio. Conversely, the use of 12 mm BFRP bars improved the flexural response and increased the ultimate moment capacity.
- All BFRP-reinforced beams maintained linear elastic behaviour up to failure and experienced sudden brittle collapse without any yielding of reinforcement. In contrast, steel-reinforced beams demonstrated ductile behaviour with distinct yielding before reaching the ultimate load. Moreover, the cracks in BFRP-reinforced specimens were mainly concentrated within the constant moment region and were characterized by wider spacing and larger crack widths.
- The analytical predictions and finite element simulations were in close agreement with the experimental observations in terms of cracking moment, ultimate moment, and moment–deflection characteristics. The obtained results indicate that the developed models are capable of accurately describing the flexural behaviour of beams reinforced with either BFRP or conventional steel bars.
- The findings of this investigation suggest that BFRP bars represent a viable alternative to steel reinforcement, particularly for structures exposed to aggressive environments where corrosion resistance, reduced self-weight, and enhanced durability are of primary importance.

REFERENCES

[1]. L. Jin, Z. Wang, R. Zhang, X. Du, Mesoscopic simulation on flexural behavior of single-way reinforced concrete slab with rebars subjected to localized corrosion, Structures 31 (2021) 815–827, https://doi.org/10.1016/j.istruc.2021.02.033.

[2]. Y.C. Ou, N.D. Nguyen, Influences of location of reinforcement corrosion on seismic performance of corroded reinforced concrete beams, Eng. Struct. 126 (2016) 210–223, https://doi.org/10.1016/j.engstruct.2016.07.048.

[3]. Tsakalidis, A. Ortega Hortelano, M. Grosso, et al., Research and innovation in bridge maintenance, inspection and monitoring, Publ. Off. Eur. Union (2019), https://doi.org/10.2760/719505.

[4]. X. Chai, H. Shang, C. Zhang, Bond behavior between corroded steel bar and concrete under sustained load, Constr. Build. Mater. 310 (2021) 125122, https:// doi.org/10.1016/j.conbuildmat.2021.125122.

[5]. X. Yu, S. Robuschi, I. Fernandez, K. Lundgren, Numerical assessment of bond-slip relationships for naturally corroded plain reinforcement bars in concrete beams, Eng. Struct. 239 (2021) 112309, https://doi.org/10.1016/j.engstruct.2021.112309.

[6]. J. Hua, F. Wang, X. Xue, H. Fan, W. Yan, Fatigue properties of bimetallic steel bar: an experimental and numerical study, Eng. Fail. Anal. 136 (2022) 106212, https://doi.org/10.1016/j.engfailanal.2022.106212.

[7]. Z. Zhang, R. Gong, H. Zhang, W. He, The Sustainability performance of reinforced concrete structures in tunnel lining induced by long-term coastal environment, Sustainability 12 (10) (2020) 3946, https://doi.org/10.3390/su12103946.

[8]. J. Cai, Q. Ran, Q. Ma, H. Zhang, K. Liu, Y. Zhou, S. Mu, Influence of a nano-hydrophobic admixture on concrete durability and steel corrosion, Materials 15 (19) (2022) 6842, https://doi.org/10.3390/ma15196842.

[9]. C. Li, L. Jiang, S. Li, Effect of limestone powder addition on threshold chloride concentration for steel corrosion in reinforced concrete, Cem. Concr. Res. 131 (2020) 106018, https://doi.org/10.1016/j.cemconres.2020.106018.

[10]. A. Al-Negheimish, R.R. Hussain, A. Alhozaimy, D.D.N. Singh, Corrosion performance of hot-dip galvanized zinc-aluminum coated steel rebars in comparison to the conventional pure zinc coated rebars in concrete environment, Constr. Build. Mater. 274 (2021) 121921, https://doi.org/10.1016/j. conbuildmat.2020.121921.

ISSN No:-2456-2165 https://doi.org/10.38124/ijisrt/26jun532

[11]. B. Goffin, N. Banthia, N. Yonemitsu, Use of infrared thermal imaging to detect corrosion of epoxy coated and uncoated rebar in concrete, Constr. Build. Mater. 263 (2020) 120162, https://doi.org/10.1016/j.conbuildmat.2020.120162.

[12]. T. Imjai, R. Garcia, M. Guadagnini, K. Pilakoutas, Strength degradation in curved Fiber-reinforced Polymer (FRP) bars used as concrete reinforcement, Polymers 12 (8) (2020) 1653, https://doi.org/10.3390/polym12081653.

[13]. L.C. Hollaway, A review of the present and future utilisation of FRP composites in the civil infrastructure with reference to their important in-service properties, Constr. Build. Mater. 24 (12) (2010) 2419–2445, https://doi.org/10.1016/j.conbuildmat.2010.04.062.

[14]. I.S. Abbood, Strut-and-tie model and its applications in reinforced concrete deep beams: a comprehensive review, Case Stud. Constr. Mater. 19 (2023), https:// doi.org/10.1016/j.cscm.2023.e02643.

[15]. Z. Sun, L. Fu, D.C. Feng, A.R. Vatuloka, Y. Wei, G. Wu, Experimental study on the flexural behavior of concrete beams reinforced with bundled hybrid steel/FRP bars, Eng. Struct. 197 (2019) 109443, https://doi.org/10.1016/j.engstruct.2019.109443.

[16]. ACI 440.1 R-15, Guide for the Design and Construction of Structural Concrete Reinforced with FRP Bars: ACI 440.1 R-15, American Concrete Institute, Farmington Hills, MI, USA, 2015.

[17]. J. Youssef, M.N. Hadi, Axial load-bending moment diagrams of GFRP reinforced columns and GFRP encased square columns, Constr. Build. Mater. 135 (2017) 550–564, https://doi.org/10.1016/j.conbuildmat.2016.12.125.

[18]. B. Zhang, H. Zhu, Z. Dong, Z. Yang, Mechanical properties and durability of FRP-reinforced coral aggregate concrete structures: a critical review, Mater. Today Commun. (2023) 105656, https://doi.org/10.1016/j.mtcomm.2023.105656.

[19]. Q. Zhao, X.L. Zhao, D. Zhang, L.P. Duan, Effects of exposure in seawater sea-sand concrete pore solution on fatigue performance of carbon FRP bars, Compos. Sci. Technol. (2023) 110418, https://doi.org/10.1016/j.compscitech.2023.110418.

[20]. K. Rashid, X. Li, Y. Xie, J. Deng, F. Zhang, Cracking behavior of geopolymer concrete beams reinforced with steel and fiber reinforced polymer bars under flexural load, Compos. Part B: Eng. 186 (2020) 107777, https://doi.org/10.1016/j.compositesb.2020.107777.

[21]. X. Liang, X. Yin, Evaluation of the flexural behavior and serviceability of engineered cementitious composite-coral aggregate concrete beams reinforced with BFRP bars, Constr. Build. Mater. 308 (2021) 124937, https://doi.org/10.1016/j.conbuildmat.2021.124937.

[22]. J. Cai, J. Pan, X. Zhou, Flexural behavior of basalt FRP reinforced ECC and concrete beams, Constr. Build. Mater. 142 (2017) 423–430, https://doi.org/10.1016/ j.conbuildmat.2017.03.087.

[23]. Z. Lu, W. Li, X. Zeng, Y. Pan, Durability of BFRP bars and BFRP reinforced seawater sea-sand concrete beams immersed in water and simulated seawater, Constr. Build. Mater. 363 (2023) 129845, https://doi.org/10.1016/j.conbuildmat.2022.129845.

[24]. V. Fiore, T. Scalici, G. Di Bella, A. Valenza, A review on basalt fibre and its composites, Compos. Part B: Eng. 74 (2015) 74–94, https://doi.org/10.1016/j. compositesb.2014.12.034.

[25]. H. Wang, A. Belarbi, Ductility characteristics of fiber-reinforced-concrete beams reinforced with FRP rebars, Constr. Build. Mater. 25 (5) (2011) 2391–2401, https://doi.org/10.1016/j.conbuildmat.2010.11.040.

[26]. C. High, H.M. Seliem, A. El-Safty, S.H. Rizkalla, Use of basalt fibers for concrete structures, Constr. Build. Mater. 96 (2015) 37–46, https://doi.org/10.1016/j. conbuildmat.2015.07.138.

[27]. J.M. Yang, K.H. Min, H.O. Shin, Y.S. Yoon, Effect of steel and synthetic fibers on flexural behavior of high-strength concrete beams reinforced with FRP bars, Compos. Part B: Eng. 43 (3) (2012) 1077–1086, https://doi.org/10.1016/j.compositesb.2012.01.044.

[28]. M.S. Issa, I.M. Metwally, S.M. Elzeiny, Influence of fibers on flexural behavior and ductility of concrete beams reinforced with GFRP rebars, Eng. Struct. 33 (5) (2011) 1754–1763, https://doi.org/10.1016/j.engstruct.2011.02.014.

[29]. F. Abed, A.R. Alhafiz, Effect of basalt fibers on the flexural behavior of concrete beams reinforced with BFRP bars, Compos. Struct. 215 (2011) 23–34, https:// doi.org/10.1016/j.compstruct.2019.02.050.

[30]. ACI 440.1R-2006. Guide for the Design and Construction of Structural Concrete Reinforced with FRP Bars: ACI 440.1 R-06. American Concrete Institute, Farmington Hills, MI, USA, 2006.

[31]. W. Ge, A. Ashour, D.F. Cao, et al., Experimental study on flexural behavior of ECC-concrete composite beams reinforced with FRP bars, Compos. Struct. 208 (2019) 454–465, https://doi.org/10.1016/j.compstruct.2018.10.026.

[32]. Z. Li, C. Ma, X. Guo, Experimental and analytical study of the flexural behavior of basalt fiber-reinforced concrete beams, Struct. Concr. (2023), https://doi.org/ 10.1002/suco.202200449.

[33]. CSA-S6-14. Canadian highway bridge design code. Rexdale (on, Canada): Canadia.

[34]. GB50608-2010, Technical specification for application of fiber reinforced composite materials in construction projects.

[35]. Q. Li, W. Guo, Y. Kuang, Parameter calculation and verification of concrete plastic damage model of ABAQUS, IOP Conf. Ser. Mater. Sci. Eng. 794 (2020) 012036, https://doi.org/10.1088/1757-899X/794/1/012036